Biosensors and Bioelectronics 154 (2020) 112053

Contents lists available at ScienceDirect

Biosensors and Bioelectronics

journal homepage: http://www.elsevier.com/locate/bios

Amyloid-beta peptide detection via aptamer-functionalized nanowire sensors exploiting single-trap phenomena

Yurii Kutovyi [a,1], Hanna Hlukhova [a,1], Nazarii Boichuk [a], Marcus Menger [b], Andreas Offenhäusser [a], Svetlana Vitusevich [a,*]

[a] Bioelectronics (ICS-8), Forschungszentrum Jülich, 52425, Jülich, Germany
[b] Fraunhofer Institute for Cell Therapy and Immunology, Branch Bioanalytics and Bioprocesses (IZI-BB), 14476, Potsdam, Germany

ARTICLE INFO

Keywords:
Alzheimer's disease
Amyloid-beta peptide
Aptamer
Silicon nanowire biosensor
Single-trap phenomena
Noise spectroscopy
Random telegraph signal noise

ABSTRACT

New highly sensitive direct methods for the early detection of peptides involved in Alzheimer's disease (AD) are required in order to prolong effective and healthy memory and thinking capabilities and also to stop the factors resulting in AD. In this contribution, we report the successful demonstration of a label-free approach for the detection of amyloid-beta (Aβ) peptides by highly selective aptamers immobilized onto the SiO_2 surface of the fabricated sensors. A modified single-stranded deoxyribonucleic acid (ssDNA) aptamer was specially designed and synthesized to detect the target amyloid beta-40 sequence (Aβ-40). Electrolyte–insulator–semiconductor (EIS) structures as well as silicon (Si) nanowire (NW) field-effect transistors (FETs) covered with a thin SiO_2 dielectric layer have been successfully functionalized with Aβ-40-specific aptamers and used to detect ultra-low concentrations of the target peptide. The binding of amyloid-beta peptides of different concentrations to the surface of the sensors varied in the range from 0.1 pg/ml to 10 μg/ml resulting in a change of the surface potential was registered by the fabricated devices. Moreover, we show that the single-trap phenomena observed in the novel Si two-layer (TL) NW FET structures with advanced characteristic parameters can be effectively used to increase the sensitivity of nanoscale sensors. The obtained experimental data demonstrate a highly sensitive and reliable detection of ultra-low concentrations of the Aβ-40 peptides. This opens up prospects for the development of real-time electrical biosensors for studying and understanding different stages of AD by utilizing Si TL NW FET structures fabricated on the basis of cost-efficient CMOS-compatible technology.

1. Introduction

Alzheimer's disease (AD) is the most common neurodegenerative disorder in humans resulting in memory loss and other cognitive problems (Citron, 2010; Nation et al., 2019). The molecular processes which take place in the brain of patients suffering from AD are irreversible and progressive leading to lethal outcomes in most of the cases. In this regard, AD is considered a very serious health problem for mankind especially in view of the increasing age of the population (Huynh and Mohan, 2017). Many efforts have been made in order to identify risk factors as well as to establish which processes lead to the onset and progression of AD. Although research is still ongoing in this direction, many studies, which are also supported by clinical trials, have demonstrated that extracellular accumulations of amyloid-beta (Aβ) plaques and intracellular neurofibrillary tangles are hallmarks of AD (Blennow et al., 2010; Citron, 2010; Hampel et al., 2010; Huynh and Mohan, 2017; Zetterberg and Schott, 2019). It has become clear that the presence and aggregation of these molecular subjects are robust evidence of pathological changes occurring in the brain during AD development. It has been revealed that among several neurotoxic Aβ isoforms, a 42-amino acid long Aβ peptide (known as Aβ-42) is a major suspect that could initiate neurodegenerative processes leading to AD (Blennow et al., 2010; Huynh and Mohan, 2017; Youn et al., 2019). While the detection of Aβ-42 is necessary to detect AD, the ratio of Aβ-42 to Aβ-40 concentrations allows the current stage of disease progression to be identified (Ghasemi et al., 2018; Hansson et al., 2007; Huynh and Mohan, 2017; Zetterberg and Schott, 2019; Zhang et al., 2019). Therefore, it is of the great importance of developing a biosensor capable of the fast, selective and highly sensitive detection of Aβ oligomers.

Up to now, different types of biosensors have been developed and

* Corresponding author.
E-mail address: s.vitusevich@fz-juelich.de (S. Vitusevich).
[1] These authors contributed equally to the work.

https://doi.org/10.1016/j.bios.2020.112053
Received 25 November 2019; Received in revised form 23 January 2020; Accepted 24 January 2020
Available online 28 January 2020

employed for the ultimate detection of various target bio-species with a limit of detection down to the single-molecule level (Kenaan et al., 2016; Macchia et al., 2019, 2018; Nguyen et al., 2014). However, there are still open questions concerning the best transducer and approach for the rapid and reliable detection of biomolecules using biosensors. At present, an enzyme-linked immunosorbent assay (ELISA) is the most commonly used technique for non-invasive detection and continuous monitoring of different bio-objects including Aβ peptides and is already available on the market (An et al., 2017; Crosnier de Lassichère et al., 2019; Jensen et al., 2000; Zhang et al., 2019; Zhou et al., 2018). However, in spite of the fact that ELISA is a highly specific and sensitive diagnostic tool, it also has several drawbacks such as biomarker labeling and utilization of bulky equipment. Such demands make the technique labor-dependent and expensive, which significantly impacts the effectiveness of such a tool for clinical practice and medical applications.

Over the past few decades, due to the fast development of nanotechnologies, bioelectronics has been transformed into being more oriented towards low-dimensional nanostructures envisioned for use as point-of-care devices. In this respect, owing to their remarkable electrical and mechanical properties, silicon nanowire-based field-effect transistors are widely considered promising candidates for transducing electrochemical signals caused by a variety of charged bio-objects including cells, proteins, DNA and viruses (Chen et al., 2011; Molaie, 2016; Patolsky et al., 2006; Zadorozhnyi et al., 2019; Zhang and Ning, 2012). However, one of the important points that have to be addressed in this regard is the electrical noise of the transducers. It has traditionally been considered that electrical noise is the limiting factor affecting biosensor performance and sensitivity (Bedner et al., 2014; Chen et al., 2015; Clément et al., 2011, 2010; Rajan et al., 2014). At the same time, the ultimate scaling down of the sizes of nanowires brings about new effects such as single-trap phenomena that can be used in order to enhance the sensitivity and efficiency of nanoscale biosensors (Gasparyan et al., 2015; Kutovyi et al., 2018b; Li et al., 2014; Pud et al., 2014). Moreover, Si nanowire-based biosensors are mass-fabrication-compatible devices, which makes them relatively cheap to produce and therefore potentially available in markets worldwide. Although they are cost-efficient and promising chemical and biological label-free transducers, Si nanowires along with other low-dimensional nanostructures still suffer from some problems including a low signal-to-noise ratio (SNR) and stability issues. To this end, the performance of such biosensors is also limited by the presence of an electrical double layer which is formed as a result of ion distribution in the ionic liquid when it comes into contact with the surface of the biosensors. Due to the ion screening effect, only biomolecules within the electrical double layer can be effectively detected by such devices (Kutovyi et al., 2018c; Lu et al., 2015). In this respect, receptor molecules responsible for the specific and selective recognition and binding of target biomolecules should not exceed the Debye screening length in order to provide effective and sensitive biosensing. One of the solutions to overcome this challenge is the utilization of shorter receptor molecules such as aptamers. In this case, the distance between the analyte and sensor surface can be about two times shorter compared to the length of commonly used antibodies. It should be noted, that label-free detection of amyloid-beta peptides using aptamers binding on a SiO_2 dielectric layer and single trap phenomena has not been reported in the literature.

In this report, we present a novel approach for Aβ peptides detection based on single-trap phenomena in newly fabricated silicon two-layer (TL) nanowire (NW) field-effect transistor (FET) structures functionalized with specially designed single-stranded deoxyribonucleic acid (ssDNA) aptamers. For the selective binding of Aβ-40 peptides, a chemical functionalization protocol enabling successful aptamer immobilization on the SiO_2 surface was developed and demonstrated. To validate the developed aptamers as highly specific receptors for Aβ-40 species involved in AD, the field-effect capacitive technique using electrolyte–insulator–semiconductor (EIS) structures was involved prior to sensing via nanowire-based devices. As a result, highly specific and label-free detection of Aβ-40 biomolecules with sub-femtomolar (fM) sensitivity was achieved. The developed single-trap-based approach for sensing of extremely low concentrations of target biomolecules allows achieving about 300% improved sensitivity compared to the standard approach utilizing measurements of current-voltage characteristics.

2. Experimental details and methods

2.1. Electrolyte–insulator–semiconductor (EIS)-based biosensor fabrication

Capacitive EIS structures were fabricated using n-doped silicon wafers with <100> orientation. The resistivity of the wafers was 5–10 Ω cm. Firstly, standard RCA cleaning of the silicon substrates was performed in order to wash away all organic and inorganic residues. After a cleaning step, the wafers were dipped into the 1%-HF solution for 2 min to remove the thin native oxide layer. Directly after HF chemical etching, the wafers were cleaned by rinsing with deionized (DI) water and a uniform 10 nm thin SiO_2 layer was grown by means of dry thermal oxidation at 950 °C. The thickness of the thermally formed oxide layer was measured for each substrate using an ellipsometer. Then, the front side of the oxidized wafers was covered with AZ 5214E photoresist layer for protection. The oxide from the rear side of the substrates was removed using a buffered oxide etch (BOE 7:1). A 200 nm thin aluminum film was then evaporated on the rear side of the wafers, and the annealing procedure was performed at 450 °C for 20 min in a forming gas atmosphere to achieve ohmic contacts between the aluminum and silicon. The substrates were then cleaned with acetone, isopropanol, and DI water. Finally, the wafers were cut into 10 × 10 mm^2 chips and used for capacitive-voltage measurements. All fabrication processes were performed at the Helmholtz Nano Facility (HNF) of Forschungszentrum Jülich.

2.2. Si TL NW FET-based biosensor fabrication

We designed and fabricated silicon two-layer nanowire structures on the basis of silicon-on-insulator (SOI) wafers with <100> Si orientation and 145 nm thick buried oxide (BOX) layer. The fabricated nanowires consist of two silicon layers with different concentrations of dopants: the first layer is the top active silicon layer of SOI wafers with an impurity concentration of 1×10^{15} cm^{-3}, while the second layer is highly doped silicon with an impurity concentration of 1×10^{17} cm^{-3}. The steps involved in the fabrication process of TL NWs are described in detail elsewhere (Kutovyi et al., 2018b, 2019). Briefly, patterns for NW structures were defined using e-beam lithography in the 20 nm thin SiO_2 layer and NWs were formed by wet chemical etching in tetramethylammonium hydroxide (TMAH) solution. Source/drain contact leads were implanted with boron atoms (energy 6 keV, dose 1×10^{15} cm^{-2}), which resulted in p-type transistor structures (p^+-p-p^+). The metallization process was then performed by evaporation of a 200 nm thick aluminum layer followed by a lift-off patterning and annealing process. To protect the metal feedlines from the electrolyte liquid environment, the passivation procedure was performed using biocompatible polyimide (PI 2545) resist. Openings in the 2 μm thick polyimide-based passivation film to provide the liquid with access to the NWs were defined by photolithography. Finally, after the fabrication processes, wafers were cut into 11 × 11 mm^2 chips, which were further wire-bonded, encapsulated with polydimethylsiloxane (PDMS) and used for the biosensing experiments.

2.3. Current-voltage and noise measurements

The current-voltage (I–V) and noise characterization of the fabricated TL nanowire structures was performed using the setups described previously (Kutovyi et al., 2018b; Petrychuk et al., 2019; Pud et al.,

2013). The I–V characteristics of the NW FETs were measured using Keithley 2430 and Keithley 2400 (Keithley Instruments Inc.) source-meter units (SMUs) allowing highly accurate electrical characterization of transistor structures with a resolution of 10 pA. Noise measurements were performed using a modernized and fully automated ultralow-noise measurement setup (PyFANS) developed in-house. The system consists of several parts including an automated voltage supply system, which allows precise electrical biasing of the device under test with an accuracy approaching 1 mV, the low-noise amplification cascade system and data acquisition system based on an Agilent U2542A SDA device as the main controlling unit. The PyFANS setup allows the time-dependent source-drain voltage fluctuations of the transistor under study to be measured with high accuracy and in real-time. To calculate the noise power spectral density (PSD) from the measured time traces, a fast Fourier transform (FFT) of the data was performed. All electrical measurements were conducted at room temperature inside an electrically shielded Faraday cage to avoid impacts from any external electromagnetic fields. All voltages were applied against the grounded source electrode. A liquid-gate voltage was applied using an external standard Ag/AgCl reference electrode.

2.4. Capacitive-voltage measurements

The capacitive-voltage (C–V) characteristics of the EIS sensors were measured using a HIOKI 3532-50 LCR impedance analyzer (HIOKI E. E. Corporation, Japan). The samples were placed into the transparent home-made measuring cell and sealed with an O-shaped resin ring defining the sensing area as about 0.37 mm^2. DC voltage was applied to the liquid gate using an Ag/AgCl reference electrode and a small superimposed AC voltage with an amplitude of 25 mV and a frequency of 1 kHz was applied to the system to measure the capacitance of the sensors. C–V characteristics were measured in a dark Faraday cage at room temperature.

2.5. Chemicals and reagents

Phosphate-buffered saline (PBS) (10 mM phosphate buffer, 2.7 mM potassium chloride, 137 mM sodium chloride, pH = 7.4), 3-glycidyloxypropyltrimethoxysilane (97-% GPTES), acetone, isopropyl alcohol, antigen Aβ-40 peptide and label-free Aβ-40-specific aptamer were used. All the above-mentioned chemicals except the aptamers were commercially purchased from Sigma-Aldrich (St. Louis, MO, USA). The 80 nt long ssDNA aptamer to Aβ-40 peptide was specifically modified by an amino group (-NH2) functionalization at the 3' end (Chakravarthy et al., 2018) and synthesized at the Fraunhofer Institute for Cell Therapy and Immunology, Potsdam, Germany.

2.6. Aptamer immobilization protocol

Structures covered with the thin SiO_2 layer were thoroughly washed with acetone, further cleaned with isopropanol and dried using N_2 gas. The devices were then treated with oxygen plasma (0.8 mbar, 50 W) for 3 min in order to activate the SiO_2 surface. Immediately after plasma treatment, the structures were salinized for 1 h in argon atmosphere (5.2 mbar) with 3- glycidyloxypropyltrimethoxysilane (GPTES) molecules in a desiccator. The devices were thoroughly rinsed with the 100%-ethanol solution to wash away unbound GPTES molecules and annealed at 100 °C to increase the strength of the molecular bonds. Finally, a PBS solution containing a 50 nM concentration of Aβ-40-specific amino-functionalized ssDNA aptamers was introduced and incubated for 2 h at room temperature. The devices were measured immediately after aptamer immobilization or stored at 4 °C until use.

3. Results and discussion

3.1. Detection of Aβ-40 biomolecules via EIS-based sensors

Firstly, the electrical detection of Aβ-40 peptides in buffer solution was performed using the above-mentioned field-effect capacitive technique, which is known as one of the most common approaches in biochemical sensing (Hlukhova et al., 2018; Poghossian et al., 2015). Since they are simple and cost-efficient in fabrication, capacitive EIS structures represent promising devices capable of the label-free sensitive detection of various charged species dissolved in a liquid. Therefore, such a technique can be effectively used for the detection and monitoring of charged biomolecules such as Aβ-40 peptides. To ensure the selectivity to target Aβ-40 peptide isoforms, EIS sensors were modified with Aβ-40-specific aptamers according to the designed protocol described above. The ssDNA aptamers were developed by a SELEX process using the biotinylated Aß-40 peptides as targets. Two control experiments involving Western blot analysis as well as an enzyme-linked oligonucleotide assay (Chakravarthy et al., 2018) have been performed to confirm the high affinity and specificity of specially designed ssDNA aptamers to Aß-40 peptide aggregates. An EIS sensor functionalized with Aβ-40-specific aptamer-based receptors is schematically shown in Fig. 1a and Fig. 1b before and after the detection of target biomolecules, respectively. The response of the sensor can be measured by monitoring the concentration-dependent shift of the C–V characteristics caused by the attachment of target peptides to the sensor surface (see Fig. 1c).

Capacitive EIS sensors consisting of Al–n-Si–SiO_2 structures with 10 nm SiO_2 functionalized with Aβ-40-specific ssDNA aptamers were employed for the detection of Aβ-40 antigens dissolved in physiological PBS solution with pH = 7.4. Firstly, reference C–V measurements were performed in the pure 10 mM PBS solution and then in solutions with different concentrations of Aβ-40 peptides. The results of the measurements are shown in Fig. 2a. With increasing Aβ-40 antigen concentration, the capacitance-voltage curves demonstrated a pronounced shift towards a higher gate voltage. The shift can be seen more clearly in Fig. 2b. Such behavior of the C–V characteristics is caused by the attachment of negatively charged Aβ-40 antigens. Since they have an isoelectric point value of 5.3 (Ghasemi et al., 2018), Aβ-40 peptides possess a net negative electrical charge in a basic solution with pH = 7.4. Therefore, the binding of Aβ-40 antigens to the surface of the Al–n-Si–SiO_2 structure induces the depletion of electrons in the space-charge region close to the semiconductor/insulator interface, which results in a decrease of space-charge capacitance in the Si for n-type EIS biosensors.

Fig. 3 shows the sensitivity of the EIS sensor to different concentrations of Aβ-40 peptides calculated as:

$$S_{(EIS)} = \frac{V_{FB}}{V_{FB0}}, \quad (1)$$

where V_{FB0} and V_{FB} denote flat band voltages of the functionalized sensor before and after the binding of target biomolecules. The flat band voltages were extracted using the slope $(d/dV_{LG})\cdot(1/C^2)$ of the linear part of $(1/C^2)$ curves recalculated from the corresponding C–V characteristics shown in Fig. 2a. The EIS sensor demonstrated a logarithmic response upon the injection of small concentrations of target biomolecules until the saturation of the signal occurred due to the charge screening effect (Nguyen et al., 2014). However, it should be noted that the EIS sensor showed the response in a wide concentration range due to the considerable sensing area of the device in comparison to small state-of-the-art nanobiosensors.

3.2. Single-trap phenomena in nanowire-based biosensors

In order to detect and prevent disease at an early stage, biological events such as the release of specific biomarkers induced by the disease

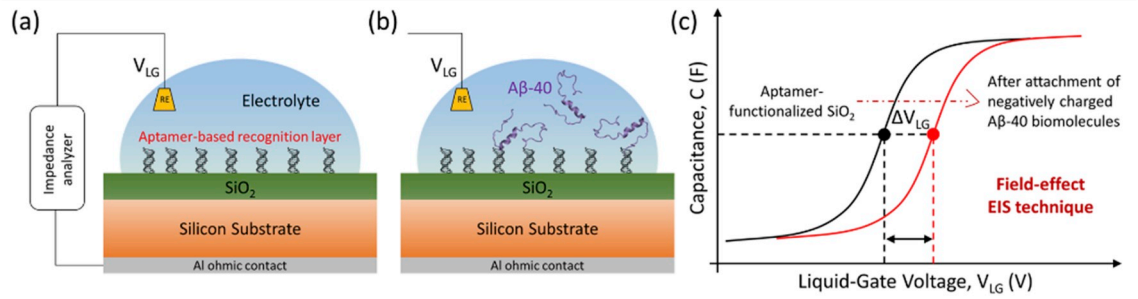

Fig. 1. Schematic illustration of the EIS sensor functionalized with an aptamer-based recognition layer before (a) and after (b) detection of Aβ-40 peptides. (c) Shift of C–V characteristics caused by the binding of target biomolecules onto the sensor surface.

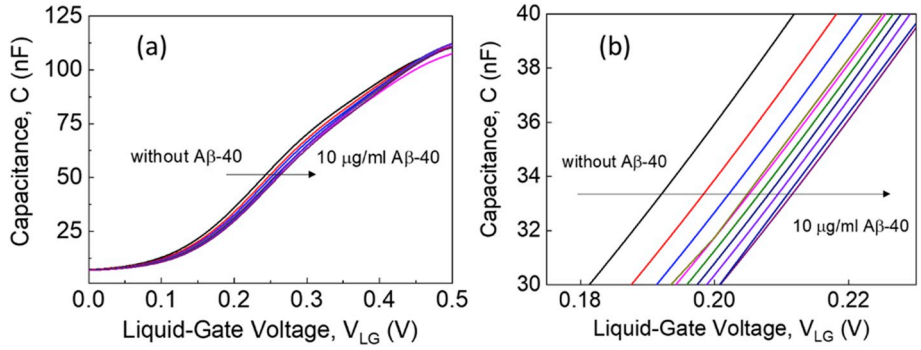

Fig. 2. (a) Capacitive-voltage curves of the Al–n-Si–SiO_2 EIS sensor measured for different concentrations of Aβ-40 peptides dissolved in physiological PBS solution with pH = 7.4. (b) A pronounced shift of C–V curves is seen in response to different concentrations of target biomolecules attached to the surface of the sensor.

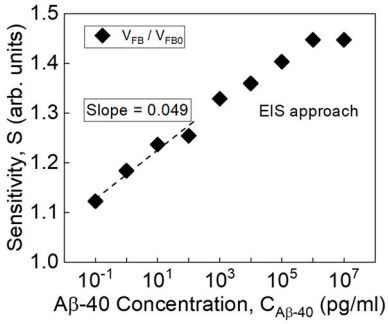

Fig. 3. Response of the EIS sensor to different concentrations of Aβ-40 peptides calculated in terms of sensitivity. The dashed line represents a linear fit of the sensor response in a small concentration range (0.1–100 pg/ml).

ideally have to be detected with single-molecule sensitivity. For this purpose, the size of the sensors has to be comparable with the biomolecules of interest. Therefore, the biosensors based on nanowires have attracted a great deal of attention in this regard due to the ultimate scaling abilities. However, with decreasing size, the limitations regarding transport and noise properties have to be established and investigated. In particular, it is traditionally considered that scaling down the sizes of biosensor devices enhances noise fluctuations affecting the performance of nanoscale biosensors. However, in the present work, we considered two-level random telegraph signal (RTS) noise fluctuations caused by a single trap in the nanowire transistor as a phenomenon highly sensitive to the biochemical processes occurring on the nanowire surface. Unlike the usual NW-based biosensors, where the threshold voltage shift is used as a signal and voltage fluctuations are considered as noise, here we demonstrate the possibility of using a single trap in a nanowire FET as a sensor in order to enhance the sensitivity of the device. For this purpose, we designed and fabricated unique silicon TL nanowire structures consisting of two silicon thin layers with different concentrations of dopants. The devices were fabricated using the protocol described above. We introduced a highly doped top epitaxial layer of silicon with advanced properties from the perspective of the single-trap phenomena (Kutovyi et al., 2018b, 2018a). A schematic illustration of the fabricated nanowire transistor with a single trap in a thin dielectric layer is shown in Fig. 4a.

Fig. 4b shows transfer curves measured for the liquid-gated Si TL NW FET with a length of 100 nm and a width of 100 nm before and after biofunctionalization with Aβ-40-specific aptamers. In these measurements, the drain current was recorded by sweeping liquid-gate voltage, while the drain-source voltage was kept constant at −20 mV to provide the linear working regime of the transistor structure. The device demonstrated transfer characteristics behavior typical of p^+-p-p^+ FETs (Bedner et al., 2014; Chen et al., 2015; Pud et al., 2014). It should be noted that the registered leakage current $I_G \leq 0.1$ nA was at least three orders of magnitude lower than the drain current within the entire range of the liquid-gate voltages applied. This confirms the high quality of the fabricated TL nanowire structures. As seen from Fig. 4b, a threshold voltage of the NW structure increased after functionalization with aptamers specific to Aβ-40 peptides. Such behavior confirms a successful immobilization of the aptamer-based biorecognition layer onto the nanowire surface.

As stated above, the device under study demonstrated pronounced RTS noise before as well as after the functionalization procedure. Two-level RTS fluctuations were observed in the subthreshold working regime of the transistor structure. Fig. 5a shows an RTS time trace with two stable states that correspond to the charge carrier being captured by or emitted from a single trap located in the gate dielectric layer close to the conductive channel. The time trace was recorded for the fabricated device at $V_{DS} = -20$ mV and $V_{LG} = -2.1$ V after the functionalization procedure. Noise PSD spectra measured at different liquid-gate voltages are plotted in Fig. 5b. As can be seen, the spectra display a Lorentzian shape reflecting characteristic RTS noise behavior caused by a single

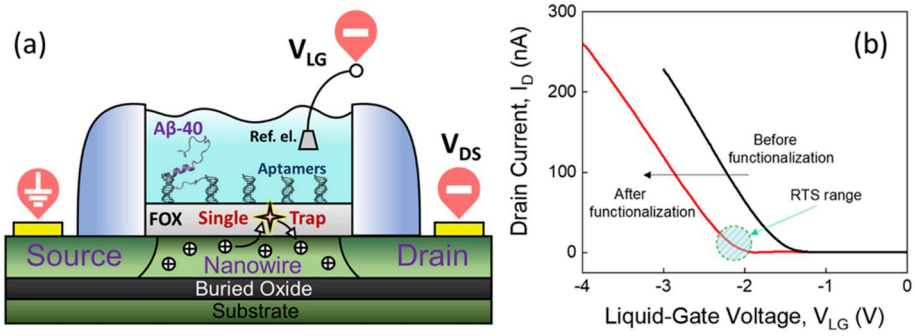

Fig. 4. (a) Sketch of a Si NW FET biosensor using the trapping/detrapping of a single carrier as a signal for the detection of target biomolecules. (b) Transfer curves of Si TL NW FET 100 nm long and 100 nm wide before and after functionalization with Aβ-40-specific ssDNA aptamers. The dashed circle shows the range of liquid-gate voltages at which pronounced RTS noise was observed.

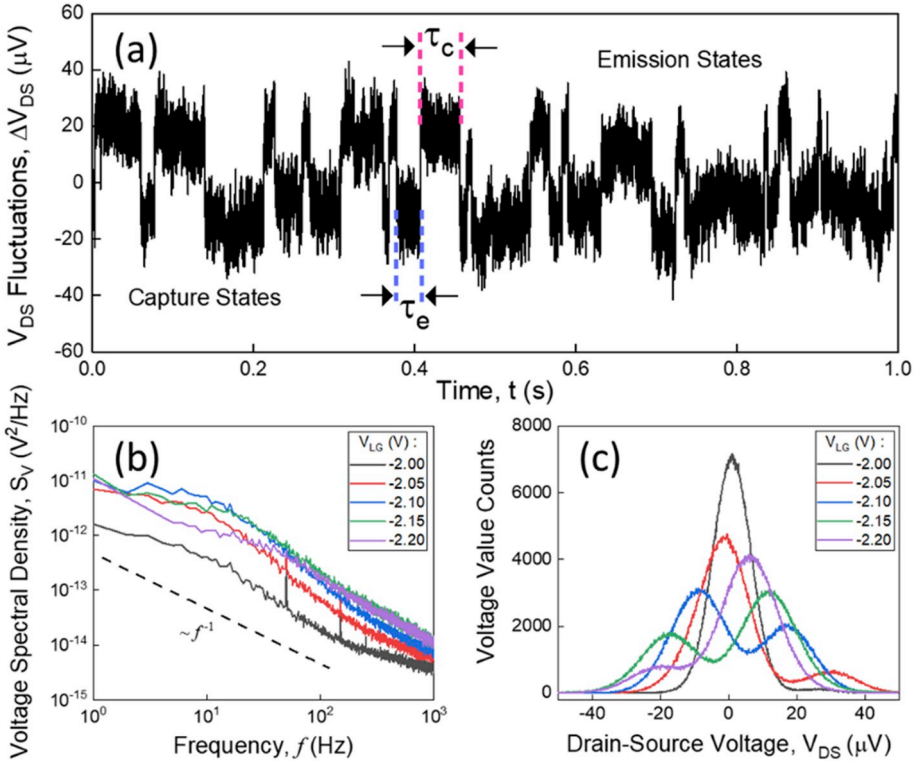

Fig. 5. (a) Two-level RTS fluctuations of drain-source voltage measured for Si TL NW FET 100 nm long and 100 nm wide after functionalization. (b) Voltage PSD at different V_{LG} showing Lorentzian behavior. (c) Histograms of the voltage fluctuations showing two Gaussians peaks.

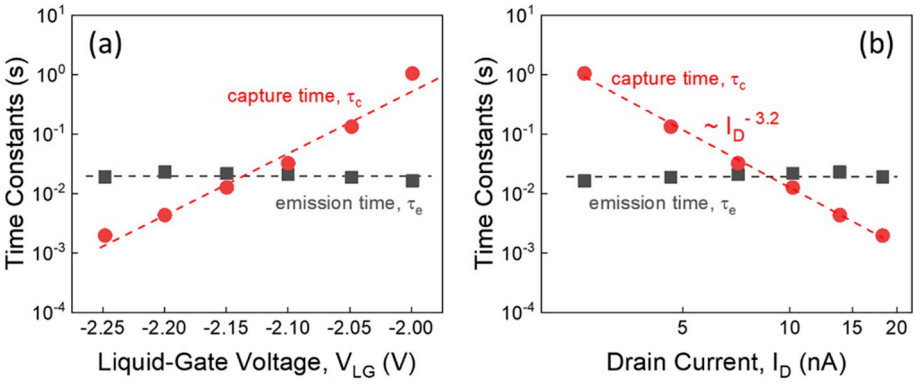

Fig. 6. Dependences of RTS characteristic time constants as a function of the liquid-gate voltage applied (a) and transistor drain current (b).

trap. The observed two-level noise fluctuations are also evident from the amplitude histograms with two Gaussian peaks corresponding to the stable states of the single trap. The histograms are shown in Fig. 5c.

The dependences of capture and emission times characterizing the measured RTS process are plotted versus the liquid-gate voltage and drain current in Fig. 6a and b, respectively. It should be noted that capture time, τ_c, and emission time, τ_e, are the average times which the system spends before carrier capture and before its emission, respectively. Characteristic capture and emission times for the single trap were extracted using a statistical method described elsewhere (Kutovyi et al., 2018b; Li et al., 2014; Yuzhelevski et al., 2000). For this purpose, the noise spectra and histograms of the time traces shown above were used. As seen from Fig. 6a, the emission time constant is almost independent of the liquid-gate voltage applied, while the capture time constant demonstrates superlinear dependence of the liquid-gate-voltage on a semi-logarithmic scale. At the same time, the two-level RTS fluctuations demonstrate enhanced capture time dependence on the drain current with a slope of (−3.2) on the logarithmic scale (see Fig. 6b). It should be noted that such behavior of RTS time constants is enhanced in liquid-gated nanowire-based FET devices (Gasparyan et al., 2015; Kutovyi et al., 2018b; Li et al., 2014; Pud et al., 2013, 2014; Vitusevich and Zadorozhnyi, 2017) compared to standard Shockley−Read−Hall (SRH) behavior with a slope equal to (−1). This reflects the fact that the single-trap phenomenon is extremely sensitive to the surface potential changes. In this respect, the trapping/detrapping dynamic of a single trap appears to be very promising for enhanced biosensing when considering characteristic capture time as a signal as will be shown below.

3.3. Detection of Aβ-40 biomolecules using single-trap phenomena approach

After RTS noise characterization, the liquid-gated TL nanowire structure functionalized with Aβ-40-specific ssDNA aptamers was further used as a sensor platform for the detection of Aβ-40 peptides dissolved in a buffer solution with pH = 7.4. In order to deliver solutions with different concentrations of Aβ-40 molecules, the drop-cast method was used. The target peptides were detected by monitoring the modulation of the transistor's drain current (standard approach) and capture time constant (single-trap approach) as the sensor was exposed to the PBS solutions with different concentrations of the analyte. For this purpose, 40-s time traces were recorded at constant $V_{DS} = -20$ mV and $V_{LG} = -2.05$ V. For each concentration of Aβ-40 peptides, the measurements were performed about 5 min after introducing analyte molecules into the buffer solution in order to achieve an equilibrium state, and thus to obtain reliable sensor output. The increase of the drain current was registered as well as the decrease of capture time upon increasing the target peptide concentration. The experimental results obtained are presented in Table 1.

The registered behavior can be explained by the electrostatic properties of Aβ-40 peptides. Since they are negatively charged in solution with pH = 7.4, Aβ-40 antigens attached to the aptamer-functionalized surface of the nanowire induce the accumulation of holes for the p-type device, which increases the probability of the trap being occupied. Thus, binding of negatively charged Aβ-40 biomolecules results in increasing drain current and decreasing characteristic capture time with increasing Aβ-40 concentration.

Table 1
Sensing parameters of the liquid-gated Si TL NW FET structure upon increasing the Aβ-40 antigens concentration.

#	Aβ-40 concentration (pg/ml)	Drain current, I_D (nA)	Capture time, τ_c (ms)
1	0	4.80	133.86
2	0.1	4.86	128.73
3	1	5.23	101.76
4	10	5.35	94.81

The sensor response in terms of the sensitivity calculated for both standard and single-trap approaches is plotted in Fig. 7. For the standard approach, when a shift of the drain current was used as a signal, the sensitivity was calculated as:

$$S_{(I_D)} = \frac{I_D}{I_{D0}} \quad , \tag{2}$$

where I_{D0} and I_D denote the drain current of the functionalized transistor before and after the binding of the target peptides. In this case, the calibration curve of the sensor can be described as a linear function with a slope of 0.051. It should be noted that the sensitivity slope is slightly higher for Aβ-40 detection in this case compared to the slope of 0.049 obtained for capacitive EIS sensors described above.

At the same time, for the single trap–approach, in which the RTS capture time constant was used as a sensing parameter, the sensitivity was defined as:

$$S_{(\tau_c)} = \frac{\tau_{c0}}{\tau_c} \, , \tag{3}$$

where τ_{c0} and τ_c stand for the average capture time constant characterizing RTS noise in the functionalized sensor before and after binding of Aβ-40 biomolecules, respectively. As can be seen from Fig. 7, the response of the sensor can be approximated as a linear function with a slope of 0.186 when considering capture time change as the signal. Such an enhanced slope value reflects the very high sensitivity of the single-trap parameters such as capture time to the surface potential changes caused by the binding of target biomolecules to the sensor surface. Therefore, in this particular case, the sensitivity of the new biosensing method was at least 3 times (or about 300%) higher for Aβ-40 detection in comparison with the conventional technique based on the monitoring of drain current changes. It should be noted that for AD diagnosis at early stages the target concentrations of Aβ biomarkers are in the range from dozens to several hundred picograms per milliliter (Yoo et al., 2017). For our developed technique, the limit of detection defined as the minimum concentration of the analyte that led to a response of the sensor is estimated to be ~20 fM. Thus, the developed technique for detection of Aβ peptides with high sensitivity at concentrations as low as 20 fM opens prospects for AD diagnosis at the early stages to monitor the dynamics of Aβ peptides and not only to predict the disease but also to apply more effective measures than medicaments to restore the balance healthy state.

4. Conclusions and outlook

Detection of Aβ peptide isoforms including Aβ-40 is extremely important for the prospects of fast and reliable medical diagnosis of Alzheimer's disease. We have successfully demonstrated the label-free and highly sensitive detection of Aβ-40 peptides using aptamer-

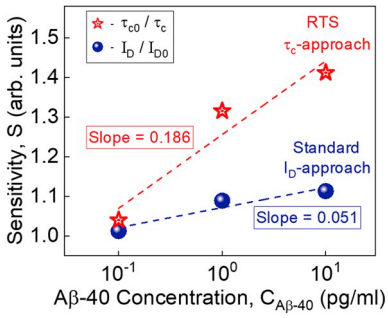

Fig. 7. Response of the sensor in terms of sensitivity calculated for the standard approach and a new RTS-based approach. The dashed lines represent linear fits with slopes indicated for both approaches.

functionalized capacitive EIS sensors as well as Si TL NW-based sensors exploiting single-trap phenomena. In order to provide high selectivity and specificity to Aβ-40 peptides over other Aβ isoforms, the devices were functionalized with specially synthesized ssDNA aptamers highly specific to Aβ-40 peptides. As a result, the fast and label-free detection of Aβ-40 molecules with high sensitivity was demonstrated. Therefore, we presented a new strategy for detection of the Aβ peptides using the single-trap phenomena allowing us to achieve about 300% enhanced sensitivity compared to EIS and standard approaches for real-time biosensing. This work can be further extended to include the detection of other Aβ peptide isoforms in real serum samples from patients suffering from Alzheimer's disease. As future work, we also plan to integrate the fabricated nanowire-based sensors exploiting single traps with a microfluidic system in order to develop a cost-efficient and robust biosensing platform.

Declaration of Competing Interest

The authors declare that they have no known competing financial interests or personal relationships that could have appeared to influence the work reported in this paper.

Acknowledgments

Yurii Kutovyi greatly appreciates a research grant no. 91618302 from the German Academic Exchange Service (DAAD). The authors also thank all the technical staff of the Helmholtz Nano Facility (HNF) of Forschungszentrum Jülich for their assistance with the fabrication of the sensors devices.

Abbreviations

AD	Alzheimer's disease
Aβ	amyloid-β
ELISA	enzyme-linked immunosorbent assay
SNR	signal-to-noise ratio
EIS	electrolyte–insulator–semiconductor structure
PI	polyimide
DI	deionized water
PBS	phosphate-buffered saline
GPTES	glycidyloxypropyltrimethoxysilane
PDMS	polydimethylsiloxane
SMU	source-meter unit
FFT	fast Fourier transform
ssDNA	single-stranded deoxyribonucleic acid
TL	two-layer
Si NW	silicon nanowire
FET	field-effect transistor
RTS	random telegraph signal
CMOS	complementary metal-oxide-semiconductor
SOI	silicon-on-insulator
TMAH	tetramethylammonium hydroxide
BOX	buried oxide
SEM	scanning electron microscope
SRH	Shockley−Read−Hall
I–V	current-voltage
C–V	capacitive-voltage

References

An, S.S.A., Lee, B.S., Yu, J.S., Lim, K., Kim, G.J., Lee, R., Kim, Shinwon, Kang, S., Park, Y. H., Wang, M.J., Yang, Y.S., Youn, Y.C., Kim, Sangyun, 2017. Dynamic changes of oligomeric amyloid β levels in plasma induced by spiked synthetic Aβ42. Alzheimer's Res. Ther. 9, 1–10. https://doi.org/10.1186/s13195-017-0310-6.

Bedner, K., Guzenko, V.A., Tarasov, A., Wipf, M., Stoop, R.L., Rigante, S., Brunner, J., Fu, W., David, C., Calame, M., Gobrecht, J., Schönenberger, C., 2014. Investigation of the dominant 1/f noise source in silicon nanowire sensors. Sensor. Actuator. B Chem. 191, 270–275. https://doi.org/10.1016/j.snb.2013.09.112.

Blennow, K., Hampel, H., Weiner, M., Zetterberg, H., 2010. Cerebrospinal fluid and plasma biomarkers in Alzheimer disease. Nat. Rev. Neurol. 6, 131–144. https://doi.org/10.1038/nrneurol.2010.4.

Chakravarthy, M., Alshamaileh, H., Huang, H., Tannenberg, R.K., Chen, S., Worrall, S., Dodd, P.R., Veedu, R.N., 2018. Development of DNA aptamers targeting low-molecular-weight amyloid-β peptide aggregates: in vitro. Chem. Commun. 54, 4593–4596. https://doi.org/10.1039/c8cc02256a.

Chen, S., Bomer, J.G., Carlen, E.T., Van Den Berg, A., 2011. Al2O3/silicon nanoISFET with near ideal nernstian response. Nano Lett. 11, 2334–2341. https://doi.org/10.1021/nl200623n.

Chen, S., Van Den Berg, A., Carlen, E.T., 2015. Sensitivity and detection limit analysis of silicon nanowire bio(chemical) sensors. Sensor. Actuator. B Chem. 209, 486–489. https://doi.org/10.1016/j.snb.2014.12.007.

Citron, M., 2010. Alzheimer's disease: strategies for disease modification. Nat. Rev. Drug Discov. 9, 387–398. https://doi.org/10.1038/nrd2896.

Clément, N., Nishiguchi, K., Dufreche, J.F., Guerin, D., Fujiwara, A., Vuillaume, D., 2011. A silicon nanowire ion-sensitive field-effect transistor with elementary charge sensitivity. Appl. Phys. Lett. 98, 96–99. https://doi.org/10.1063/1.3535958.

Clément, N., Nishiguchi, K., Fujiwara, A., Vuillaume, D., 2010. One-by-one trap activation in silicon nanowire transistors. Nat. Commun. 1, 8. https://doi.org/10.1038/ncomms1092.

Crosnier de Lassichère, C., Duc Mai, T., Taverna, M., 2019. Antibody-free detection of amyloid beta peptides biomarkers in cerebrospinal fluid using capillary isotachophoresis coupled with mass spectrometry. J. Chromatogr. A 1601, 350–356. https://doi.org/10.1016/j.chroma.2019.05.006.

Gasparyan, F., Zadorozhnyi, I., Vitusevich, S., 2015. Single trap in liquid gated nanowire FETs: capture time behavior as a function of current. J. Appl. Phys. 117 https://doi.org/10.1063/1.4919816.

Ghasemi, F., Reza Hormozi-Nezhad, M., Mahmoudi, M., 2018. Label-free detection of β-amyloid peptides (Aβ40 and Aβ42): a colorimetric sensor array for plasma monitoring of Alzheimer's disease. Nanoscale 10, 6361–6368. https://doi.org/10.1039/c8nr00195b.

Hampel, H., Frank, R., Broich, K., Teipel, S.J., Katz, R.G., Hardy, J., Herholz, K., Bokde, A.L.W., Jessen, F., Hoessler, Y.C., Sanhai, W.R., Zetterberg, H., Woodcock, J., Blennow, K., 2010. Biomarkers for alzheimer's disease: Academic, industry and regulatory perspectives. Nat. Rev. Drug Discov. 9, 560–574. https://doi.org/10.1038/nrd3115.

Hansson, O., Zetterberg, H., Buchhave, P., Andreasson, U., Londos, E., Minthon, L., Blennow, K., 2007. Prediction of Alzheimer's disease using the CSF Aβ42/Aβ40 ratio in patients with mild cognitive impairment. Dement. Geriatr. Cognit. Disord. 23, 316–320. https://doi.org/10.1159/000100926.

Hlukhova, H., Menger, M., Offenhäusser, A., Vitusevich, S., 2018. Highly sensitive aptamer-based method for the detection of cardiac biomolecules on silicon dioxide surfaces. MRS Adv. 3, 1535–1541. https://doi.org/10.1557/adv.2018.332.

Huynh, R.A., Mohan, C., 2017. Alzheimer's disease: biomarkers in the genome, blood, and cerebrospinal fluid. Front. Neurol. 8, 15. https://doi.org/10.3389/fneur.2017.00102.

Jensen, M., Hartmann, T., Engvall, B., Wang, R., Uljon, S.N., Sennvik, K., Näslund, J., Muehlhauser, F., Nordstedt, C., Beyreuther, K., Lannfelt, L., 2000. Quantification of Alzheimer amyloid beta peptides ending at residues 40 and 42 by novel ELISA systems. Mol. Med. 6, 291–302.

Kenaan, A., Nguyen, T.D., Dallaporta, H., Raimundo, J.M., Charrier, A.M., 2016. Subpicomolar iron sensing platform based on functional lipid monolayer microarrays. Anal. Chem. 88, 3804–3809. https://doi.org/10.1021/acs.analchem.5b04834.

Kutovyi, Y., Zadorozhnyi, I., Handziuk, V., Boichuck, N., Hlukhova, H., Petrychuk, M., 2018a. Single electron dynamics in liquid-gated two-layer silicon nanowire Structures : towards biosensing with enhanced sensitivity. In: SSDM Conference. Tokyo, pp. 659–660.

Kutovyi, Y., Zadorozhnyi, I., Handziuk, V., Hlukhova, H., Boichuk, N., Petrychuk, M., Vitusevich, S., 2019. Temperature-dependent noise and transport in silicon two-layer nanowire FETs. Phys. Status Solidi Basic Res. 256, 1–6. https://doi.org/10.1002/pssb.201800636.

Kutovyi, Y., Zadorozhnyi, I., Handziuk, V., Hlukhova, H., Boichuk, N., Petrychuk, M., Vitusevich, S., 2018b. Liquid-gated two-layer silicon nanowire FETs: evidence of controlling single-trap dynamic processes. Nano Lett. 18, 7305–7313. https://doi.org/10.1021/acs.nanolett.8b03508.

Kutovyi, Y., Zadorozhnyi, I., Hlukhova, H., Handziuk, V., Petrychuk, M., Ivanchuk, A., Vitusevich, S., 2018c. Origin of noise in liquid-gated Si nanowire troponin biosensors. Nanotechnology 29. https://doi.org/10.1088/1361-6528/aaaf9e.

Li, J., Pud, S., Petrychuk, M., Offenhaeusser, A., Vitusevich, S., 2014. Sensitivity enhancement of Si nanowire field effect transistor biosensors using single trap phenomena. Nano Lett. 14, 3504–3509. https://doi.org/10.1021/nl5010724.

Lu, M.-P., Vire, E., Montès, L., 2015. Ionic screening effect on low-frequency drain current fluctuations in liquid-gated nanowire FETs. Nanotechnology 26, 495501. https://doi.org/10.1088/0957-4484/26/49/495501.

Macchia, E., Manoli, K., Holzer, B., Di Franco, C., Ghittorelli, M., Torricelli, F., Alberga, D., Mangiatordi, G.F., Palazzo, G., Scamarcio, G., Torsi, L., 2018. Single-molecule detection with a millimetre-sized transistor. Nat. Commun. 9 https://doi.org/10.1038/s41467-018-05235-z.

Macchia, E., Manoli, K., Holzer, B., Di Franco, C., Picca, R.A., Cioffi, N., Scamarcio, G., Palazzo, G., Torsi, L., 2019. Selective single-molecule analytical detection of C-reactive protein in saliva with an organic transistor. Anal. Bioanal. Chem. 411, 4899–4908. https://doi.org/10.1007/s00216-019-01778-2.

Molaie, M., 2016. Field-effect transistor nanobiosensors: state-of-the-art and key challenges as point of care testing devices. Nanomed. J 3, 69–82. https://doi.org/10.7508/nmj.2016.02.001.

Nation, D.A., Sweeney, M.D., Montagne, A., Sagare, A.P., D'Orazio, L.M., Pachicano, M., Sepehrband, F., Nelson, A.R., Buennagel, D.P., Harrington, M.G., Benzinger, T.L.S., Fagan, A.M., Ringman, J.M., Schneider, L.S., Morris, J.C., Chui, H.C., Law, M., Toga, A.W., Zlokovic, B.V., 2019. Blood–brain barrier breakdown is an early biomarker of human cognitive dysfunction. Nat. Med. 25, 270–276. https://doi.org/10.1038/s41591-018-0297-y.

Nguyen, T.D., Labed, A., El Zein, R., Lavandier, S., Bedu, F., Ozerov, I., Dallaporta, H., Raimundo, J.M., Charrier, A.M., 2014. A field effect transistor biosensor with a γ-pyrone derivative engineered lipid-sensing layer for ultrasensitive Fe 3+ ion detection with low pH interference. Biosens. Bioelectron. 54, 571–577. https://doi.org/10.1016/j.bios.2013.11.051.

Patolsky, F., Zheng, G., Lieber, C.M., 2006. Fabrication of silicon nanowire devices for ultrasensitive, label-free, real-time detection of biological and chemical species. Nat. Protoc. 1, 1711–1724. https://doi.org/10.1038/nprot.2006.227.

Petrychuk, M., Zadorozhnyi, I., Kutovyi, Y., Karg, S., Riel, H., Vitusevich, S., 2019. Noise spectroscopy to study the 1D electron transport properties in InAs nanowires. Nanotechnology 30, 305001. https://doi.org/10.1088/1361-6528/ab175e.

Poghossian, A., Bäcker, M., Mayer, D., Schöning, M.J., 2015. Gating capacitive field-effect sensors by the charge of nanoparticle/molecule hybrids. Nanoscale 7, 1023–1031. https://doi.org/10.1039/c4nr05987e.

Pud, S., Gasparyan, F., Petrychuk, M., Li, J., Offenhäusser, A., Vitusevich, S.A., 2014. Single trap dynamics in electrolyte-gated Si-nanowire field effect transistors. J. Appl. Phys. 115 https://doi.org/10.1063/1.4883757.

Pud, S., Li, J., Petrychuk, M., Feste, S., Vitusevich, S., Danilchenko, B., Offenhäusser, A., Mantl, S., 2013. Modulation phenomena in Si nanowire field-effect transistors characterized using noise spectroscopy and gamma radiation technique. J. Appl. Phys. 113 https://doi.org/10.1063/1.4795603.

Rajan, N.K., Brower, K., Duan, X., Reed, M.A., 2014. Limit of detection of field effect transistor biosensors: effects of surface modification and size dependence. Appl. Phys. Lett. 104, 130–133. https://doi.org/10.1063/1.4867025.

Vitusevich, S., Zadorozhnyi, I., 2017. Noise spectroscopy of nanowire structures: fundamental limits and application aspects. Semicond. Sci. Technol. 32 https://doi.org/10.1088/1361-6641/aa5cf3.

Yoo, Y.K., Kim, J., Kim, G., Kim, Y.S., Kim, H.Y., Lee, S., Cho, W.W., Kim, S., Lee, S.M., Lee, B.C., Lee, J.H., Hwang, K.S., 2017. A highly sensitive plasma-based amyloid-β detection system through medium-changing and noise cancellation system for early diagnosis of the Alzheimer's disease. Sci. Rep. 7 https://doi.org/10.1038/s41598-017-09370-3.

Youn, Y.C., Kang, S., Suh, J., Park, Y.H., Kang, M.J., Pyun, J.M., Choi, S.H., Jeong, J.H., Park, K.W., Lee, H.W., An, S.S.A., Dominguez, J.C., Kim, S., 2019. Blood amyloid-β oligomerization associated with neurodegeneration of Alzheimer's disease. Alzheimer's Res. Ther. 11, 1–8. https://doi.org/10.1186/s13195-019-0499-7.

Yuzhelevski, Y., Yuzhelevski, M., Jung, G., 2000. Random telegraph noise analysis in time domain. Rev. Sci. Instrum. 71, 1681. https://doi.org/10.1063/1.1150519.

Zadorozhnyi, I., Hlukhova, H., Kutovyi, Y., Handziuk, V., Naumova, N., Offenhaeusser, A., Vitusevich, S., 2019. Towards pharmacological treatment screening of cardiomyocyte cells using Si nanowire FETs. Biosens. Bioelectron. 137, 229–235. https://doi.org/10.1016/j.bios.2019.04.038.

Zetterberg, H., Schott, J., 2019. Biomarkers for Alzheimer's disease beyond amyloid and tau. Nat. Med. 25, 201–203. https://doi.org/10.1038/s41591-019-0347-0.

Zhang, G.J., Ning, Y., 2012. Silicon nanowire biosensor and its applications in disease diagnostics: a review. Anal. Chim. Acta 749, 1–15. https://doi.org/10.1016/j.aca.2012.08.035.

Zhang, Y., Figueroa-Miranda, G., Lyu, Z., Zafiu, C., Willbold, D., Offenhäusser, A., Mayer, D., 2019. Monitoring amyloid-B proteins aggregation based on label-free aptasensor. Sensor. Actuator. B Chem. 288, 535–542. https://doi.org/10.1016/j.snb.2019.03.049.

Zhou, Y., Li, C., Li, X., Zhu, X., Ye, B., Xu, M., 2018. A sensitive aptasensor for the detection of β-amyloid oligomers based on metal-organic frameworks as electrochemical signal probes. Anal. Methods 10, 4430–4437. https://doi.org/10.1039/c8ay00736e.